ARTICLES

Atomic structure of a voltage-dependent K^+ channel in a lipid membrane-like environment

Stephen B. Long[1]†, Xiao Tao[1], Ernest B. Campbell[1] & Roderick MacKinnon[1]

Voltage-dependent K^+ (Kv) channels repolarize the action potential in neurons and muscle. This type of channel is gated directly by membrane voltage through protein domains known as voltage sensors, which are molecular voltmeters that read the membrane voltage and regulate the pore. Here we describe the structure of a chimaeric voltage-dependent K^+ channel, which we call the 'paddle-chimaera channel', in which the voltage-sensor paddle has been transferred from Kv2.1 to Kv1.2. Crystallized in complex with lipids, the complete structure at 2.4 ångström resolution reveals the pore and voltage sensors embedded in a membrane-like arrangement of lipid molecules. The detailed structure, which can be compared directly to a large body of functional data, explains charge stabilization within the membrane and suggests a mechanism for voltage-sensor movements and pore gating.

Whether found on voltage-dependent ion channels[1], voltage-dependent proton channels[2,3] or voltage-regulated enzymes[4], amino acid sequence conservation indicates that the basic structural unit of the voltage sensor is conserved. The voltage sensor is a membrane-protein domain with charged amino acids embedded within the membrane electric field. It undergoes conformational change associated with displacement of charged amino acids, detectable through electrical measurements as gating charge[5]. The voltage sensor is therefore an electromechanical coupling device in which the membrane voltage biases the conformation of the domain, which in turn is coupled to the pore of an ion channel or to the active site of an enzyme.

X-ray crystallographic studies of Kv channels have described the voltage-sensor architecture, but many fundamental questions remain unanswered[6–8]. These questions concern the distance over which the gating charges move, and the physical and chemical principles by which the charges are stabilized within the membrane. Ultimately, these questions must be addressed using atomic structures in a membrane setting. To this end, our laboratory has explored three-dimensional protein crystals containing lipid–detergent mixtures to achieve membrane-protein structures in a membrane-like environment.

Structure of the paddle-chimaera channel

We have determined the structure of a modified rat Kv1.2 K^+ channel in which the voltage-sensor paddle, a helix–turn–helix structural motif comprising the S3b and S4 helices, has been replaced by the voltage-sensor paddle from the rat Kv2.1 K^+ channel (Fig. 1a)[9,10]. Construction of the paddle-chimaera channel was based on the demonstration that the voltage-sensor paddle is transferable among voltage sensors of different origin[11]. The crystals, grown in a mixture of detergents and phospholipids, are unrelated to the Kv1.2 crystal and are formed with unique protein–protein contacts[7]. Diffraction data were collected to 2.4 ångström (Å), and phases were determined by molecular replacement using the Kv1.2 crystal structure as a search model. Electron density corresponding to the voltage-sensor paddle is shown (Fig. 1b). The maps were of high quality throughout, except for a segment connecting the cytoplasmic T1 domain to the first transmembrane region. This segment, built as a polyglycine helix in the Kv1.2 structure, is probably extended over part of its length (Supplementary Fig. 1). The final model, refined to an R_{free} of 0.24, includes all amino acids within the transmembrane region, 16 total or partial lipid molecules per subunit, an $NADP^+$ cofactor and 193 water molecules (molecule 1, Methods).

An α-carbon trace of the transmembrane region is shown, with the voltage-sensor paddles coloured red and a segment of the S1–S2 connection coloured pale blue (Fig. 1c). The voltage-sensor paddle is tilted away from the central axis of the voltage sensor, towards the lipid membrane, such that it makes minimal contact with the remainder of the channel. One entire face of the voltage-sensor paddle is exposed to the lipid membrane. The region of minimal contact corresponds to the largest transferable segment of the paddle defined in ref. 11. The S1–S2 loop segment (pale blue) contains a short α helix that rests between two halves of the voltage sensor (that is, the voltage-sensor paddle defining one half and the S1 and S2 helices defining the other half). The paddle-chimaera channel produces voltage-dependent K^+ currents in lipid membranes that are very similar to those in the Kv1.2 channel (Fig. 1d, chimaera). Removal of the pale blue segment within the S1–S2 loop (Fig. 1c) has little effect on voltage-dependent opening (Fig. 1d, ΔS1–S2 loop).

Conservation of structure in K^+ channels

The Shaker K^+ channel and other closely related eukaryotic Kv channels have been the subjects of K^+ conduction and selectivity studies, whereas the *Streptomyces lividans* K^+ channel (KcsA) has provided the most detailed structural description of a K^+ channel[12–15]. Eukaryotic Shaker-like Kv channels and KcsA have almost identical K^+ selectivity filters (Fig. 2a). The root mean square deviation for all atoms in the filter (sequence TVGYG) is 0.25 Å. This extent of deviation probably corresponds to the limit of accuracy with which the crystallographic data define the atomic positions at 2.4 Å resolution[16]. At 2.4 Å, the paddle-chimaera channel shows that the selectivity filter of Kv channels is structurally identical to inward rectifier K^+ channels and KcsA (conductive conformation) to within a few tenths of an ångström[15,16].

Figure 2b shows a superposition of transmembrane regions for the paddle chimaera and Kv1.2. The voltage-sensor paddles of Kv1.2 and

[1]Howard Hughes Medical Institute, Laboratory of Molecular Neurobiology and Biophysics, Rockefeller University, 1230 York Avenue, New York, New York 10065, USA. †Present address: Structural Biology Program, Memorial Sloan-Kettering Cancer Center, Box 414, 1275 York Avenue, New York, New York 10065, USA.

the paddle chimaera differ by 27 amino acids over the 32 amino acids substituted (Fig. 1a), but nevertheless their overall conformations are the same. In particular, the tilted position of the voltage-sensor paddle away from the central axis of the voltage sensor is very similar in the two structures. These two channels form different crystal lattices with unique protein contacts. Because the voltage sensor adopts the same conformation in the settings of different crystal contacts, it is unlikely that these contacts dictate the conformation of the voltage sensor.

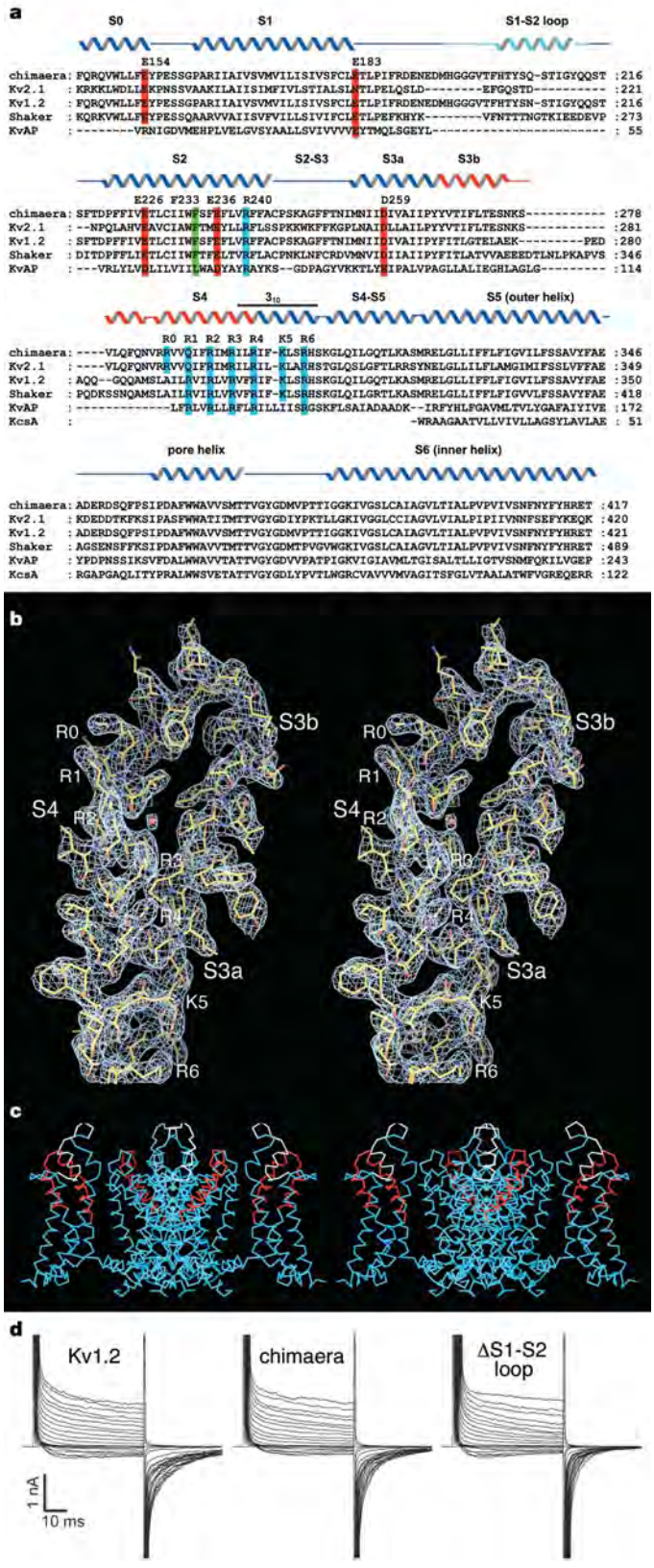

Figure 2c shows a superposition of the voltage sensor from the paddle-chimaera channel and the isolated voltage sensor of KvAP, a prokaryotic Kv channel[6]. For visual clarity, the S1–S2 loop of the paddle chimaera is not shown. The structures have been aligned to minimize the deviation between the S1 and S2 helices of the two channels. Specific positively and negatively charged amino acids almost superimpose, indicating that these voltage sensors are closely related members of the voltage-sensor structural family. However, there are informative structural differences between them. The sharp kink at a proline residue, which demarcates S3a and S3b in the paddle-chimaera channel, is replaced by a complete break and partial unwinding of the S3 helix in KvAP. The S2–S3 turn, also known as the membrane interface anchor[6,8], is lifted 'higher' in KvAP, and the voltage-sensor paddles have different degrees of rotation. The paddle units themselves, however, can be superimposed as shown (Fig. 2d). The structural similarities between the paddle-chimaera and KvAP voltage sensors—in particular the good superposition of charged amino acids—imply that the voltage sensors are in related conformational states. The structural differences are compatible with the idea that the voltage-sensor paddle is mobile with respect to the S1 and S2 helices[8,17,18].

Lipid interactions

Biochemical purification and crystallization of the Kv1.2 K^+ channel required a mixture of phospholipids and detergents[7]. The paddle-chimaera structure provides an explanation for the lipid requirement. Multiple complete and/or partial lipid molecules surround the channel in the crystal lattice (Fig. 3a, b and Supplementary Fig. 2). The extended alkyl chains of partial lipid molecules are distinguishable from detergent molecules because none of the detergents used in the preparation contained extended alkyl chains. Several aspects of the lipid molecules in the crystal are worth comment. First, there is a bilayer-like arrangement near the protein surface, with the outer leaflet particularly well formed (Fig. 3a). This observation suggests that the mixed micelle is a better membrane mimic than a pure detergent micelle. Second, lipid molecules are most dense in the concave hemi-circles between the voltage sensors (Fig. 3b). The hemi-circles reflect the very complex shape of a Kv channel, in which voltage-sensor domains protrude like appendages mostly surrounded by lipid membrane. By filling in space, the lipid molecules are an integral part of this membrane-protein structure and probably confer stability to it. Third, the lipid head groups reside at different 'membrane depths' with respect to the channel (Fig. 3a). This may, in part, reflect the fact that the bilayer-like micelle is not a true membrane. However, it may also reflect the fact that a membrane protein can perturb the positions of nearby lipid molecules away from the

Figure 1 | Paddle-chimaera channel. a, Sequence alignment of the paddle-chimaera channel, rat Kv2.1 (GI, 24418849), rat Kv1.2 (GI, 1235594), Shaker Kv (GI, 13432103), KvAP (GI, 5104624) and KcsA (GI, 61226909) transmembrane regions. Secondary structure elements are indicated above the sequences: pale blue, the region removed in the ΔS1–S2 loop construct; red, the S3b–S4 region of Kv2.1 inserted into the Kv1.2 channel (dark blue). Residues discussed in the text are highlighted red (negatively charged), blue (positively charged) and green (phenylalanine 233). **b**, Stereo representation of electron density (wire mesh) for the S3–S4 region ($2F_o$–F_c, calculated from 50–2.4 Å using phases from the final model and contoured at 1.2σ). The structure of the protein (sticks) and two water molecules (red spheres, adjacent to R2 and 'behind' R4) are shown. **c**, Overall structure of the transmembrane region (α-carbon trace in stereo, coloured as in **a**). **d**, Channel activation. Currents are shown of wild-type Kv1.2 (left), the paddle-chimaera channel (middle), and the paddle-chimaera channel ΔS1–S2 loop (right), without subtracting leak and capacitive currents. Voltage pulses, –110 mV to 110 mV; ΔV = 10 mV; holding potential, –110 mV, stepping back to –90 mV.

more even plane of molecules normally associated with a pure lipid bilayer. The unusually positioned lipid molecules make specific favourable interactions with the ion channel, and probably influence its structure and function[19]. An example of a displaced phospholipid molecule is shown wedged between the voltage sensor and the S4–S5 linker, a region of the channel that couples voltage-sensor motions to pore gating (Fig. 3c)[18,20,21].

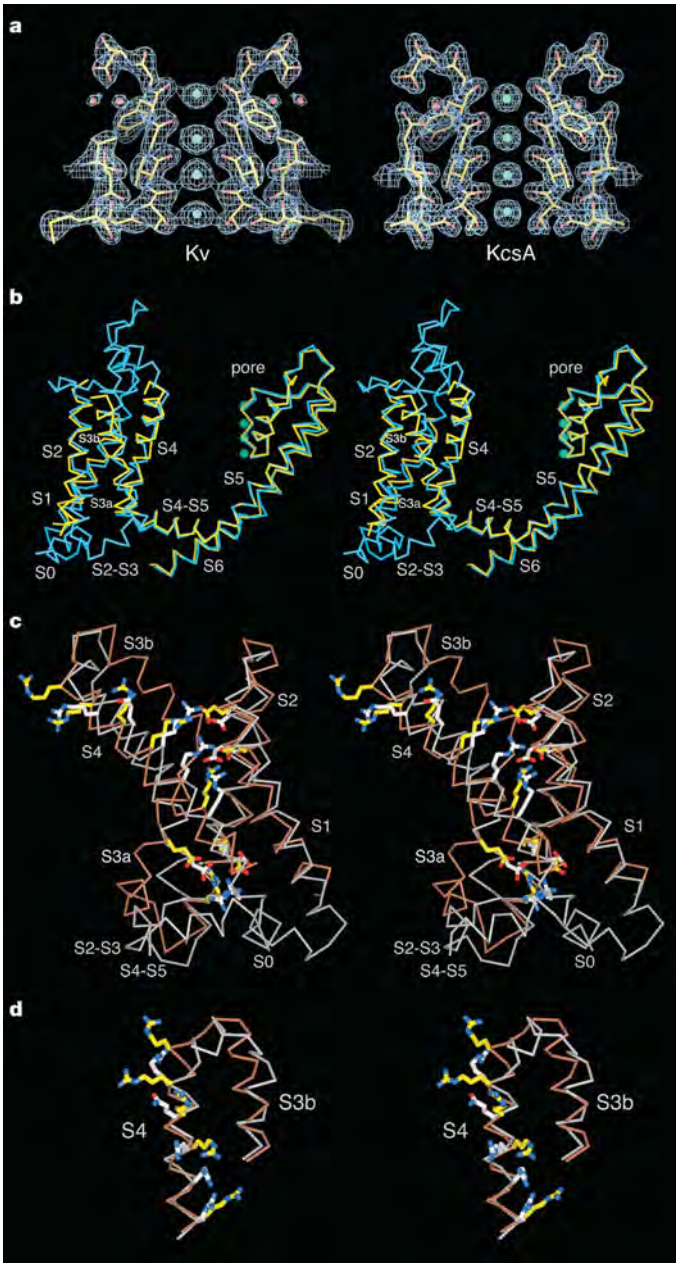

Figure 2 | Comparison of the paddle-chimaera channel with other K^+ channel structures. **a**, K^+ selectivity filter of the paddle-chimaera channel (Kv, left) compared with that of KcsA (PDB accession number, 1K4C, right). For clarity, two of the four subunits are shown (yellow sticks). Electron density (wire mesh, $2F_o$–F_c, 2.5σ contour), K^+ ions (green spheres) and water molecules (red spheres) are shown. **b**, Comparison with the Kv1.2 structure (**b**, **c** and **d** are shown in stereo). The α-carbon trace of Kv1.2 (yellow, PDB accession number, 2A79) and paddle chimaera structures (cyan) are superimposed. **c**, Superposition of the paddle chimaera voltage sensor (grey α-carbon trace, with the S1–S2 connecting loop removed for visual clarity), and the isolated voltage sensor of KvAP[6] (brown α-carbon trace, PDB accession number, 1ORS). Positively and negatively charged amino acids are shown as sticks (KvAP, yellow; paddle chimaera, white). **d**, Superposition of the S3b–S4 voltage sensor paddles from KvAP and the chimaera channel (coloured as in **c**).

Detailed structure of the voltage sensor

Figure 4a shows a voltage sensor and an S4–S5 linker helix (white α-carbon trace) relative to the pore (cyan α-carbon trace). The gate of the ion-conduction pore, which is formed by the crossing of four S6 inner helices (one from each subunit)[22], adopts an open conformation in the paddle-chimaera channel. The S4–S5 linker helix engages the S6 helix and is angled in a manner consistent with the channel's open conformation, as was observed in the Kv1.2 structure[18]. The S1 helix makes specific contacts with the pore helix and the S5 helix (green side chains). Hanatoxin-interacting residues are located on the lipid-exposed face of the voltage-sensor paddle (red side chains)[23]. Figure 4b shows a voltage sensor and an S4–S5 linker helix viewed from the pore, with the yellow side chains from Fig. 4a and water molecules coloured according to atom type. The tilted position of the voltage-sensor paddle (S3b–S4) away from the S1 and S2 helices creates an external aqueous cleft in the voltage sensor that penetrates approximately 10 Å below the level of the membrane surface.

Negatively charged amino acids in the voltage sensor fall into two clusters: an external negative cluster consisting of glutamate 183 (S1 helix) and glutamate 226 (S2 helix), and an internal negative cluster consisting of glutamate 154 (S0 helix), glutamate 236 (S2 helix) and aspartate 259 (S3a helix) (Fig. 4b). These negative clusters are separated by approximately 15 Å (distance between nearest charges: glutamate 226 and glutamate 236). The external negative cluster is located in the external aqueous cleft. The internal negative cluster, in particular amino acids glutamate 236 and aspartate 259, are part of a buried network of charged amino acids, not exposed to aqueous solution, located approximately 10 Å from the intracellular membrane surface. Phenylalanine 233, located near the midpoint of the membrane, separates the external and internal negative clusters (Fig. 4b, green). Among Kv channels, the amino acids forming the negative clusters are very conserved as glutamate or aspartate. Phenylalanine 233 is the single most conserved amino acid in Kv

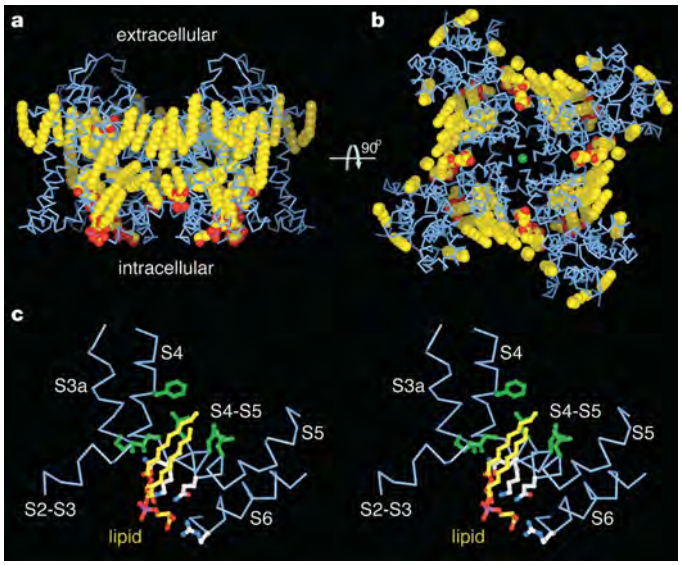

Figure 3 | Lipids in the structure. **a**, Side view of the transmembrane region showing lipid molecules (CPK representation, coloured according to atom type: yellow, carbon; red, oxygen; magenta, phosphorous) and the channel (blue α-carbon trace). **b**, View from the extracellular side of the membrane with potassium shown as a green sphere. The lipid observed at the subunit–subunit interface in the structure of KcsA[15] (PDB accession number, 1K4C) is also observed in the paddle-chimaera channel (prominent red headgroup, nearest the centre). **c**, Detailed interactions of a lipid (yellow and red sticks) bound between the voltage sensor and the S4–S5 linker helix, in stereo. Amino acids that interact with the lipid are shown as sticks and are coloured according to chemical nature (green, hydrophobic residues; white, hydrophilic residues with nitrogen (blue) and oxygen (red) atoms).

channels outside the selectivity filter (Fig. 1a). KvAP is a rare example in which leucine is present in place of phenylalanine.

Positively charged amino acids on S4 are labelled in Fig. 4b according to an alignment with the Shaker K^+ channel (Fig. 1a). Kv2.1 has a glutamine residue (glutamine 290 in the paddle chimaera) corresponding to the first S4 arginine in Shaker (R1) and an additional preceding arginine labelled R0. Positively charged amino acids K5 and R6 form ionized hydrogen bonds with the internal negative cluster, whereas R3 and R4 form ionized hydrogen bonds with the external negative cluster. R0, R1 and R2 are positioned to interact favourably with the lipid phosphodiester layer, a mixed lipid–water environment and the water environment of the external aqueous cleft, respectively.

The side chains of R0, R1, R2, R3 and R4 are all effectively in or close to the extracellular solution, where we expect to find them in the open conformation of the voltage sensor. Four aspects of the voltage-sensor structure account for the extracellular disposition of these amino acids. First, the tilted paddle creates the external cleft into which the extracellular solution penetrates. Second, the side chains of R3 and R4 are drawn towards the surface by electrostatic attraction to the external negative cluster. Third, the S4 helix adopts a 3_{10}-helix hydrogen-bonding pattern 'below' position 296 (R3)[24]. The 3_{10} helix is associated with a translation of 2.0 Å per amino acid, in contrast to 1.5 Å for an α helix[25]. Consequently, over a 10-amino-acid segment (position 297 to 306) the S4 helix is 5 Å longer than it would be if it were entirely α-helical. In effect, the 'bottom' of the S4 helix is stretched towards the extracellular side, allowing the voltage-sensor paddle to reside closer to the extracellular solution. Fourth, the short helix in the S2–S3 turn leading into S3a and the S4–S5 linker helix leading out of S4 are both angled in a manner to suggest that the entire S3 plus S4 'half' of the voltage sensor is displaced towards the extracellular solution relative to the S1 plus S2 'half' (Fig. 4a, b).

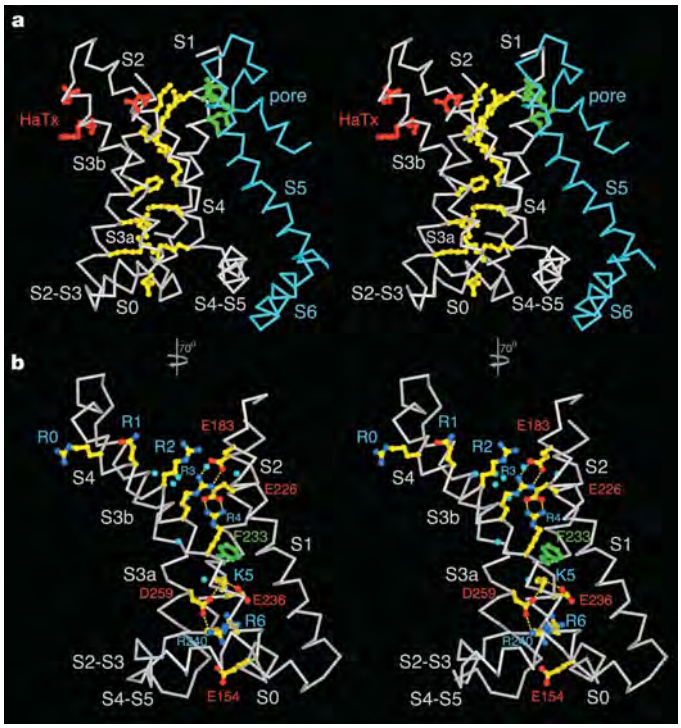

Figure 4 | Details of the voltage sensor. a, Stereo representation of a voltage sensor and the S4–S5 linker helix (white α-carbon trace) in relation to the pore (cyan α-carbon trace). The view is from the side (extracellular solution 'above' and intracellular solution 'below'). Select residues are shown as sticks and are coloured as indicated in the text. **b**, Voltage sensor and S4–S5 linker helix (white α-carbon trace) viewed from the pore. Yellow side chains from **a** and water molecules are now coloured according to atom type (yellow, carbon; blue, nitrogen; red, oxygen; green, phenylalanine 233; cyan, water). Ionized hydrogen bonds between basic and acidic residues are indicated by dashed yellow lines.

Inferring motion from functional data

For the Shaker and Kv2.1 K^+ channels, opening is coupled to displacement of 3 or 4 charge units per voltage sensor (12 to 16 charges per channel) across the membrane-voltage difference[26–29]. The roughly equal total gating charge measured for Shaker and Kv2.1 suggests that R0 in Kv2.1 might compensate for the absence of a charge at R1 (Figs 1a and 4b)[30]. In Shaker, R1, R2, R3 and R4 each contribute approximately a single charge and K5 contributes approximately half a charge[28,29]. The crystal structure of the open conformation is consistent with these electrical measurements if all five positions reach an internal location in the closed conformation: the first four would thus move from outside to inside and the fifth would move from its midway point (about half way between the base of the external cleft and the internal solution) to inside (Fig. 4b). 'Outside' and 'inside' in these measurements refer to regions of electrical isopotential with bulk solution, which are a function of the detailed geometry of the voltage sensor and the surrounding lipid molecules.

Gating-associated-protein motions have been assessed using methanethiosulfonate (MTS) reactivity of site-directed cysteines in the Shaker K^+ channel (Fig. 5a, b)[31]. Red, yellow and blue spheres correspond to positions accessible from the outside, not accessible from either side, and accessible from the inside, respectively. In the open conformation (Fig. 5a), accessibility is compatible with the crystal structure: yellow spheres (inaccessible) are distributed across a buried 17 Å stretch extending from the base of the external cleft to the internal solution. This entire stretch becomes exposed to internal MTS reagents (blue spheres) in the closed conformation (Fig. 5b), implying that closure is associated with a large translation of S4 towards the internal solution and/or a wide opening of the voltage sensor to the inside (enough to permit entry of MTS reagents all the way to R3).

Histidine substitutions imply motion by their state-dependent ability to transfer protons across the voltage sensor (Fig. 5c)[32,33]. At R4, a histidine substitution causes a proton current through the voltage sensor in the open conformation. In the crystal structure (open conformation), the R4 α-carbon (magenta sphere) is at the level of phenylalanine 233 (green). A histidine side chain at this location is well positioned to flip above and below the phenylalanine side chain by rapid rotamer exchange, allowing protons to be transferred from the base of the external cleft (outside) to protonatable side chains below. The charged network below the phenylalanine forms a continuous hydrogen-bonding network through which protons could diffuse all the way to the intracellular solution. Histidine substitution at R1 (red sphere) also creates a proton current, but only when the voltage sensor adopts its closed conformation. A simple interpretation is that voltage-sensor closure moves the R1 α-carbon next to phenylalanine 233 (that is, to the position of the R4 α-carbon in the open conformation). Such a motion would correspond to an S4 translation of approximately 15 Å. Histidine substitution at R2 and R3 (orange spheres) creates a proton shuttle that has maximum throughput at 50% open probability, implying that these positions are alternately exposed to one side or the other, depending on the conformation of the voltage sensor. This behaviour is expected if, indeed, R1 resides near phenylalanine 233 in the closed conformation.

In KvAP, motions have been inferred by accessibility experiments in which biotin, tethered at specific positions, is captured by avidin in solution (Fig. 5d)[34]. The main difference between this type of accessibility and MTS accessibility is that avidin is too large to enter clefts in the voltage sensor, so reactivity requires the tethered biotin to reach the membrane surface. Red, yellow and blue spheres correspond to positions accessible from the outside, not accessible from either side, and accessible from the inside, respectively, in either the

opened or the closed conformation. Blue spheres on the S4 helix (near R4), which are near the extracellular surface in the open conformation, must move to the level of the other blue spheres near the intracellular surface when the channel closes. This would necessitate a translation of at least 15 Å.

These different electrical and biochemical measurements interpreted in light of the crystal structure are consistent, and point to an S4 displacement of about 15 Å and a large reorganization of the voltage sensor associated with gating.

Hypothesis for the voltage-sensing mechanism

Electrophysiological measurements show that the paddle-chimaera channel is open at 0 mV (Fig. 1d). In the crystal, which is at 0 mV and provides a membrane-like environment, the channel also adopts an open conformation. Closing the voltage sensor requires a strong electric field associated with a negative (intracellular) membrane voltage to force the positive gating charges inward. Electrical measurements indicate that the charges get most of the way across the voltage difference during this transition[28,29]. Until the structure of a closed conformation is solved, the details of how this occurs will remain unknown; however, the pictures in Fig. 6 illustrate one way in which this could happen. In the depiction, the voltage-sensor paddle moves relative to the S1 and S2 helices. This movement translates the region of S4 centred on the gating charges ~15 Å towards the intracellular side, approximately half the membrane hydrophobic core thickness of a pure phosphatidylcholine bilayer (30 Å)[35]. Because of the shape of the voltage sensor and its effect on membrane thickness, 15 Å would be sufficient to transfer the charges from the electrical outside to the electrical inside.

This model is silent on many details, but further inspection of the crystal structure (Fig. 4b) stimulates several new ideas concerning voltage-sensor motion. First, the S2–S3 turn looks as if it could reorganize its structure, enabling movements within the voltage sensor (Fig. 4a, b). This turn is conserved in length and in certain amino acids (Fig. 1a), but is one of the least-studied regions in Kv channels. Second, the contact between S1 and the pore (Fig. 4a, green) is well positioned to hold the S1–S2 half of the voltage sensor static relative to the pore. Without this contact, motions of the voltage-sensor paddle relative to S1 and S2 might not transmit force as effectively to the S4–S5 linker helix. Ultimately, sensor closure must push down on the S4–S5 linker helix to constrict the pore until it is closed, as depicted (Fig. 6)[18]. Third, the 3_{10}-helical intracellular half of S4, in addition to allowing the voltage-sensor paddle to reside closer to the extracellular solution in the open state (by 'stretching' S4), also directs arginine and lysine side chains that occur at every third position to the same helical face[25]. In the crystal structure, in which the channel is open, the 3_{10} helix directs R4, K5 and R6 away from the membrane and into the sensor (Fig. 4b). It is possible that during closure, as the paddle moves inward, the zone of 3_{10}-helical secondary structure shifts as a moving segment along S4 in a wave-like fashion. Such a 'concertina effect' would turn arginine residues away from the lipid membrane and towards the inside of the voltage sensor as they cross the centre of the hydrophobic core without necessitating rigid body rotation of the S4 helix.

The crystal structure also provides new ideas concerning charge stabilization during gating. Two negatively charged clusters near the external and internal aspects of the voltage sensor capture and stabilize gating charges on either side (Fig. 4b). But how are charges stabilized while crossing between these clusters? Perhaps the most intriguing aspect of the voltage sensor is a complete absence of charge near the membrane centre for a hydrophobic zone of roughly 10 Å between the negative clusters (Fig. 4b). This zone contains a phenylalanine residue (position 233 in the paddle-chimaera channel) in 355

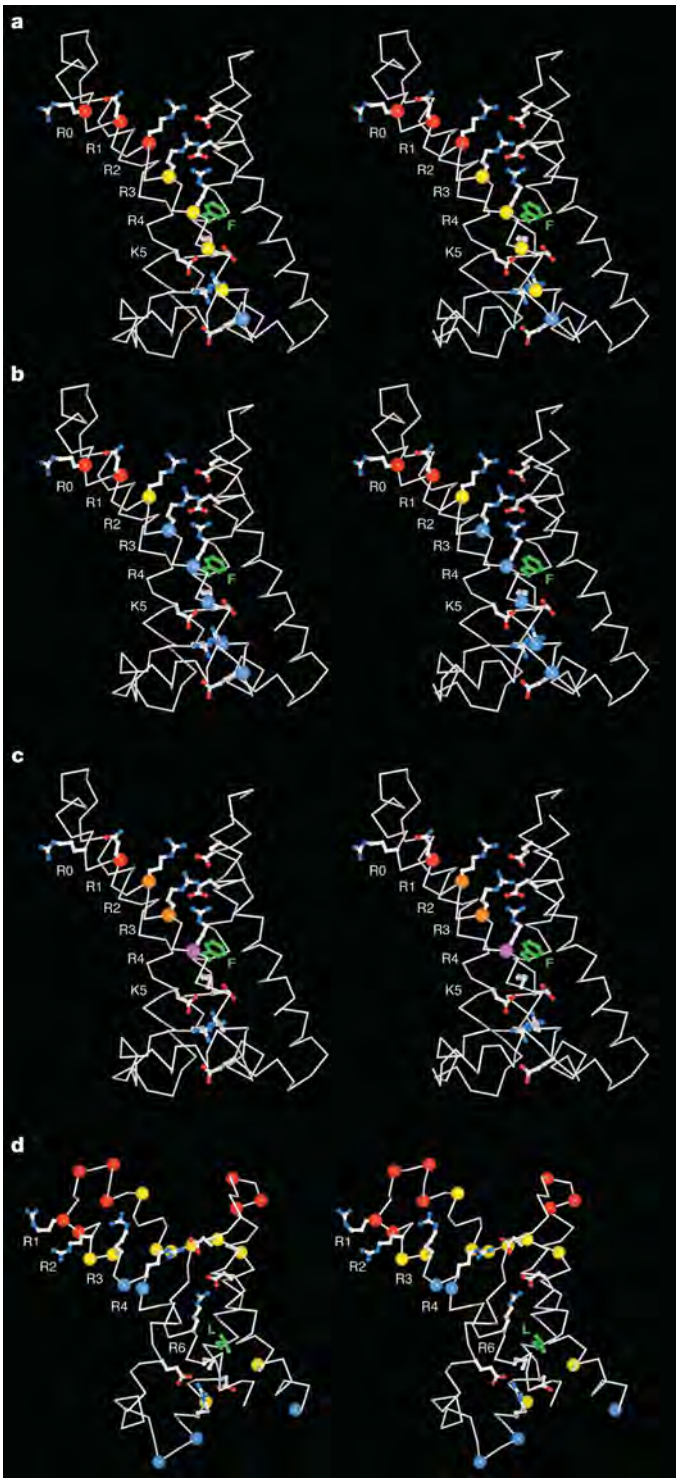

Figure 5 | Mapping of biochemical data on the voltage sensor. In **a**–**c**, the voltage sensor and S4–S5 linker helix (white α-carbon trace) are viewed from the pore (extracellular solution 'above' and intracellular solution 'below'), in stereo. Phenylalanine 233 (F) is coloured green. Basic and acidic residues (sticks) are coloured according to atom type: white, carbon; red, oxygen; blue, nitrogen. **a**, **b**, MTS reactivity of site-directed cysteine residues introduced into Shaker on the S4 helix[31] mapped on the crystal structure. **a**, MTS accessibility in the open (depolarized) state. **b**, MTS accessibility in the closed (polarized) state. **c**, Histidine substitutions at four positions on the S4 helix[32,33] mapped on the structure (coloured spheres as described in the text). **d**, Biotin–avidin accessibility data mapped on the structure of the isolated voltage sensor of KvAP (PDB accession number, 1ORS)[34]. The view of voltage sensor (S1–S4, white α-carbon trace) is the same as that for the paddle chimaera in **a**–**c** (superposition as in Fig. 2c). KvAP has a leucine (L, green side chain) at the position corresponding to phenylalanine 233 in the chimaera paddle. Coloured spheres indicate positions described in the text.

out of 360 Kv channels, and therefore we call it the 'phenylalanine gap' separating the external and internal negative clusters. Other than weak stabilization that might occur transiently through cation-π interactions with the phenylalanine[36], the phenylalanine gap seems energetically unfavourable for a positive charge. The arginine side chains must apparently flip between charge clusters on their way across the membrane. We speculate that the absence of polar groups in the central zone might prevent proton transfer across the membrane, which would lead to cell acidification, and it might also create an energy barrier for the arginines, which would favour a switch-like transition between closed and opened conformations.

Discussion

The KvAP crystal structures and functional studies led to the hypothesis of a voltage-sensor paddle—a helix–turn–helix unit that moves at the protein–lipid interface[6,17]. It was proposed that acidic amino acids would help to stabilize positive charges on the paddle as it moves within the membrane to control pore gating[17]. The Kv1.2 crystal structure demonstrated the lipid-surrounded, independent domain property of the voltage sensor, partial shielding of charges from the membrane, and the mechanical connection by which conformational changes in the sensor are transmitted to the pore through the S4–S5 linker helix[7,18]. Here, at high resolution and in a membrane-like environment, the paddle-chimaera channel reveals atomic interactions: arginine exposure to the membrane at the phosphodiester layer, charge stabilization by external and internal negative clusters inside the sensor, a phenylalanine gap across which the arginine residues must transit, and the possibility of a concertina effect in which an α- to 3_{10}-helical secondary structure transition could turn arginine residues away from the lipid membrane as paddle displacement moves them across the hydrophobic core.

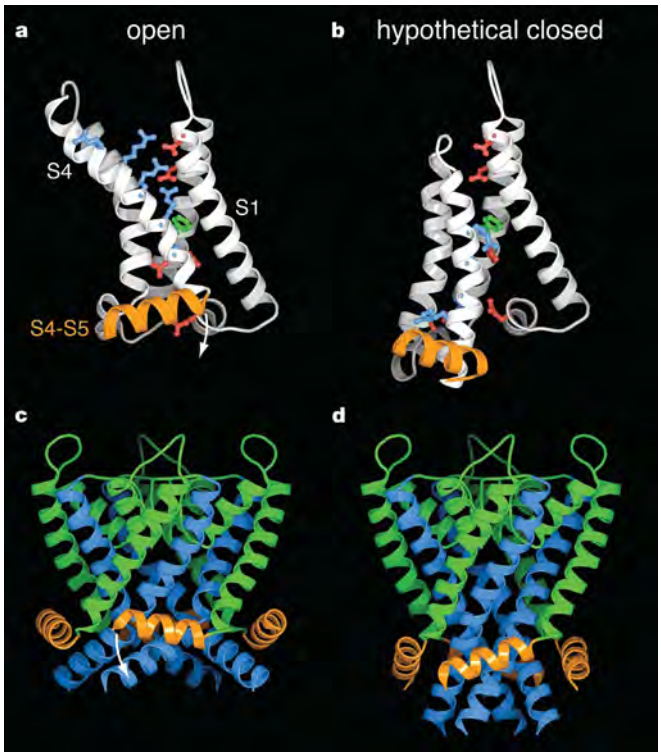

Figure 6 | Hypothetical mechanism of voltage-dependent gating. **a**, Representation of the voltage sensor and S4–S5 linker helix from the crystal structure (open conformation). Helices are drawn as ribbons. The view is from the pore, as in Fig. 5, with the extracellular solution 'above' and the intracellular solution 'below'. The gating charges (R1 to K5) are shown as blue sticks. Negatively charged residues in the external and internal clusters are red; the phenylalanine in the middle is green. The positively charged residues reach 'outward' towards the extracellular solution. **b**, Depiction of a hypothetical closed conformation of the voltage sensor. The S1 and S2 helices are hypothesized to maintain their position, whereas the S3–S4 paddle has moved inward. The positive charges on S4 now reach towards the intracellular solution, and are stabilized through interactions with the internal negative cluster. The α-carbon position of R1 is adjacent to the phenylalanine, representing a displacement perpendicular to the plane of the membrane of approximately 15 Å relative to its location in the open structure (**a**). The inward displacement of the S4 helix pushes down on the N-terminal end of the S4–S5 linker helix, causing it to tilt towards the intracellular side and to close the pore. **c**, Depiction of the open conformation of the S4–S5 linker helices and pore from the crystal structure. The S4–S5 linker helices (orange) rest on the S6 helices (blue ribbons) near the intracellular side. **d**, A hypothetical model of the S4–S5 linker helices and pore in a closed conformation based on the crystal structure of a closed potassium channel pore (KcsA, PDB accession number, 1K4C)[18].

METHODS SUMMARY

The paddle-chimaera channel with a His_{10} tag at the amino terminus was co-expressed with the rat β2.1 subunit in *Pichia pastoris* and purified using metal affinity chromatography and gel filtration. Protein crystals were grown from hanging drops at pH 8.5, and contain the detergents 6-cyclohexyl-1-hexyl-β-D-maltoside (Cymal-6), 7-cyclohexyl-1-heptyl-β-D-maltoside (Cymal-7) and CHAPS and the lipids POPC (1-palmitoyl-2-oleoyl-*sn*-glycero-3-phosphocholine), POPE (1-palmitoyl-2-oleoyl-*sn*-glycero-3-phosphoethanolamine) and POPG (palmitoyl-2-oleoyl-*sn*-glycero-3-[phospho-rac-(1-glycerol)]). X-ray data (50–2.4 Å, space group $P42_12$) were collected at beamline X29 (Brookhaven National Synchrotron Light Source (NSLS)). The structure was determined by molecular replacement using the structure of Kv1.2 in complex with its β subunit as a search model (PDB accession number, 2A79). There are two channel subunits and two β subunits in the asymmetric unit, giving rise to two tetrameric assemblies (identified as molecule 1 and molecule 2 in the text). The model was built using O[37] and was refined with CNS[38] to an R_{free} of 24.4%. Crystallographic data and refinement statistics are shown in the Supplementary Information.

The purified channels were reconstituted into POPE:POPG lipid vesicles by dialysis. Planar lipid bilayer experiments were performed as described previously[39,40]. Electrical measurements were carried out using the voltage-clamp method in whole-cell mode. Charybdotoxin (CTX) (1 μM, ref. 41) was used to block channels in one orientation while channels in the other orientation were being recorded.

Full Methods and any associated references are available in the online version of the paper at www.nature.com/nature.

Received 8 August; accepted 17 September 2007.

1. Noda, M. *et al.* Expression of functional sodium channels from cloned cDNA. *Nature* **322**, 826–828 (1986).
2. Ramsey, I. S., Moran, M. M., Chong, J. A. & Clapham, D. E. A voltage-gated proton-selective channel lacking the pore domain. *Nature* **440**, 1213–1216 (2006).
3. Sasaki, M., Takagi, M. & Okamura, Y. A voltage sensor-domain protein is a voltage-gated proton channel. *Science* **312**, 589–592 (2006).
4. Murata, Y., Iwasaki, H., Sasaki, M., Inaba, K. & Okamura, Y. Phosphoinositide phosphatase activity coupled to an intrinsic voltage sensor. *Nature* **435**, 1239–1243 (2005).
5. Armstrong, C. M. & Bezanilla, F. Charge movement associated with the opening and closing of the activation gates of the Na^+ channels. *J. Gen. Physiol.* **63**, 533–552 (1974).
6. Jiang, Y. *et al.* X-ray structure of a voltage-dependent K^+ channel. *Nature* **423**, 33–41 (2003).
7. Long, S. B., Campbell, E. B. & MacKinnon, R. Crystal structure of a mammalian voltage-dependent Shaker family K^+ channel. *Science* **309**, 897–903 (2005).
8. Lee, S. Y., Lee, A., Chen, J. & MacKinnon, R. Structure of the KvAP voltage-dependent K^+ channel and its dependence on the lipid membrane. *Proc. Natl Acad. Sci. USA* **102**, 15441–15446 (2005).
9. Stuhmer, W. *et al.* Molecular basis of functional diversity of voltage-gated potassium channels in mammalian brain. *EMBO J.* **8**, 3235–3244 (1989).
10. Frech, G. C., VanDongen, A. M., Schuster, G., Brown, A. M. & Joho, R. H. A novel potassium channel with delayed rectifier properties isolated from rat brain by expression cloning. *Nature* **340**, 642–645 (1989).
11. Alabi, A. A., Bahamonde, M. I., Jung, H. J., Kim, J. I. & Swartz, K. J. Portability of paddle motif function and pharmacology in voltage sensors. *Nature* doi:10.1038/nature06266 (this issue).
12. Kamb, A., Iverson, L. E. & Tanouye, M. A. Molecular characterization of Shaker, a *Drosophila* gene that encodes a potassium channel. *Cell* **50**, 405–413 (1987).
13. Tempel, B. L., Papazian, D. M., Schwarz, T. L., Jan, L. Y. & Jan, Y. N. Sequence of a probable potassium channel component encoded at Shaker locus of *Drosophila*. *Science* **237**, 770–775 (1987).

14. Pongs, O. *et al.* Shaker encodes a family of putative potassium channel proteins in the nervous system of *Drosophila*. *EMBO J.* **7,** 1087–1096 (1988).
15. Zhou, Y., Morais-Cabral, J. H., Kaufman, A. & MacKinnon, R. Chemistry of ion coordination and hydration revealed by a K^+ channel–Fab complex at 2.0 Å resolution. *Nature* **414,** 43–48 (2001).
16. Nishida, M., Cadene, M., Chait, B. T. & MacKinnon, R. Crystal of a Kir3.1–prokaryotic Kir channel chimera. *EMBO J.* **26,** 4005–4015 (2007).
17. Jiang, Y., Ruta, V., Chen, J., Lee, A. & MacKinnon, R. The principle of gating charge movement in a voltage-dependent K^+ channel. *Nature* **423,** 42–48 (2003).
18. Long, S. B., Campbell, E. B. & MacKinnon, R. Voltage sensor of Kv1.2: structural basis of electromechanical coupling. *Science* **309,** 903–908 (2005).
19. Schmidt, D., Jiang, Q. X. & MacKinnon, R. Phospholipids and the origin of cationic gating charges in voltage sensors. *Nature* **444,** 775–779 (2006).
20. Lu, Z., Klem, A. M. & Ramu, Y. Coupling between voltage sensors and activation gate in voltage-gated K+ channels. *J. Gen. Physiol.* **120,** 663–676 (2002).
21. Sukhareva, M., Hackos, D. H. & Swartz, K. J. Constitutive activation of the Shaker Kv channel. *J. Gen. Physiol.* **122,** 541–556 (2003).
22. Jiang, Y. *et al.* The open pore conformation of potassium channels. *Nature* **417,** 523–526 (2002).
23. Swartz, K. J. & MacKinnon, R. Mapping the receptor site for hanatoxin, a gating modifier of voltage-dependent K^+ channels. *Neuron* **18,** 675–682 (1997).
24. Laskowski, R. A. MacArthur M. W., Moss, D. S. & Thornton, J. M. PROCHECK: a program to check the stereochemical quality of protein structures. *J. Appl. Cryst.* **26,** 283–291 (1993).
25. Branden, C. & Tooze, J. *Introduction to Protein Structure* page 15 (Garland Publishing Inc., New York, 1999).
26. Zagotta, W. N., Hoshi, T., Dittman, J. & Aldrich, R. W. Shaker potassium channel gating. II: transitions in the activation pathway. *J. Gen. Physiol.* **103,** 279–319 (1994).
27. Schoppa, N. E., McCormack, K., Tanouye, M. A. & Sigworth, F. J. The size of gating charge in wild-type and mutant Shaker potassium channels. *Science* **255,** 1712–1715 (1992).
28. Aggarwal, S. K. & MacKinnon, R. Contribution of the S4 segment to gating charge in the Shaker K^+ channel. *Neuron* **16,** 1169–1177 (1996).
29. Seoh, S. A., Sigg, D., Papazian, D. M. & Bezanilla, F. Voltage-sensing residues in the S2 and S4 segments of the Shaker K^+ channel. *Neuron* **16,** 1159–1167 (1996).
30. Islas, L. D. & Sigworth, F. J. Voltage sensitivity and gating charge in Shaker and Shab family potassium channels. *J. Gen. Physiol.* **114,** 723–742 (1999).
31. Larsson, H. P., Baker, O. S., Dhillon, D. S. & Isacoff, E. Y. Transmembrane movement of the Shaker K^+ channel S4. *Neuron* **16,** 387–397 (1996).
32. Starace, D. M. & Bezanilla, F. A proton pore in a potassium channel voltage sensor reveals a focused electric field. *Nature* **427,** 548–553 (2004).
33. Starace, D. M. & Bezanilla, F. Histidine scanning mutagenesis of basic residues of the S4 segment of the shaker K^+ channel. *J. Gen. Physiol.* **117,** 469–490 (2001).
34. Ruta, V., Chen, J. & MacKinnon, R. Calibrated measurement of gating-charge arginine displacement in the KvAP voltage-dependent K^+ channel. *Cell* **123,** 463–475 (2005).
35. King, G. I. & White, S. H. Determining bilayer hydrocarbon thickness from neutron diffraction measurements using strip-function models. *Biophys. J.* **49,** 1047–1054 (1986).
36. Burley, S. K. & Petsko, G. A. Amino–aromatic interactions in proteins. *FEBS Lett.* **203,** 139–143 (1986).
37. Jones, T. A., Zou, J. Y., Cowan, S. W. & Kjeldgaard, M. Improved methods for building protein models in electron density maps and the location of errors in these models. *Acta Crystallogr.* **A47,** 110–119 (1991).
38. Brunger, A. T. *et al.* Crystallography & NMR system: a new software suite for macromolecular structure determination. *Acta Crystallogr.* **D54,** 905–921 (1998).
39. Ruta, V., Jiang, Y., Lee, A., Chen, J. & MacKinnon, R. Functional analysis of an archeabacterial voltage-dependent K^+ channel. *Nature* **422,** 180–185 (2003).
40. Miller, C. *Ion Channel Reconstitution* (Plenum, New York, 1986).
41. Miller, C., Moczydlowski, E., Latorre, R. & Phillips, M. Charybdotoxin, a protein inhibitor of single Ca^{2+}-activated K^+ channels from mammalian skeletal muscle. *Nature* **313,** 316–318 (1985).

Supplementary Information is linked to the online version of the paper at www.nature.com/nature.

Acknowledgements We thank A. L. MacKinnon for CTX and discussions, S.-Y. Lee and T. Muir for discussions, K. Swartz for providing information enabling the chimaera construction, and the staff at beamline X29, NSLS, Brookhaven National Laboratory. R.M. is an Investigator in the Howard Hughes Medical Institute. This work was supported by the NIH (R.M.).

Author Information The X-ray crystallographic coordinates and structure factor data have been deposited in the Protein Data Bank under accession number 2R9R. Reprints and permissions information is available at www.nature.com/reprints. Correspondence and requests for materials should be addressed to R.M. (mackinn@mail.rockefeller.edu).

METHODS

Cloning, expression and purification. A gene encoding the paddle-chimaera channel was constructed using standard DNA techniques as follows. The full-length rat Kv1.2 gene[9] (GI, 1235594) with an N-terminal His_{10} tag and a thrombin protease cleavage site (MAH_{10}GLVPRGSMT(X_n)stop) was ligated into the multiple cloning site of the pPICZ-C vector (Invitrogen Life Technologies). Five amino acid substitutions were made to remove a glycosylation site and to reduce sensitivity to oxidation (N207Q, C31S, C32S, C434S and C482S). The region of the Kv1.2 gene encoding the S3b–S4 paddle was replaced with the corresponding region of rat Kv2.1 to yield the protein sequence VAIIPYYVTIFLTESNKSVLQFQNVRRVVQIFRIMRILRIFK (in which the Kv2.1 sequence is underlined). This construct encoding the paddle-chimaera channel was combined with a pPICZ-C vector containing the rat β2.1 gene (residues 36–367) as described[7]. This vector, containing both the Kv1.2–Kv2.1 paddle-chimaera channel and the β2.1 subunits, was used to transform yeast. Transformation of *P. pastoris*, expression, and cobalt affinity purification were performed as described[7].

After elution from the cobalt affinity column, the protein was concentrated to approximately 20 mg ml^{-1}, and was further purified on a Superdex-200 gel-filtration column. The buffer used for gel filtration consisted of: 150 mM KCl, 20 mM TRIS-HCl, pH 7.5, 3 mM Cymal-6 (anagrade, Anatrace), 3 mM Cymal-7 (anagrade, Anatrace), 1 mM EDTA, 2 mM Tris[2-carboxyethyl]phosphine (TCEP), 10 mM DTT and 0.1 mg ml^{-1} lipid (3:1:1, POPC:POPE:POPG, obtained from Avanti). The mixture of detergents used (Cymal-6 and Cymal-7) improved the diffraction quality of the crystals. The gel-filtration fraction eluting between 11 ml and 12 ml showed Kv1.2 and β2.1 proteins in correct ratio on Coomassie-stained SDS–PAGE. Protein was concentrated to 10 mg ml^{-1} (using a Centricon-50, Millipore), mixed with crystallization solution (1 μl protein plus 1 μl solution), supplemented with 0.1 μl CHAPS detergent additive (80 mM Hampton Research) and crystallized using the hanging-drop method over reservoirs containing 0.1 ml crystallization solution at 20 °C. The crystallization solution contained 28–36% PEG 400, 50 mM TRIS-HCl, pH 8.5. Crystals appeared within 5 days and were approximately 200 μm in each dimension.

ΔS1–S2 loop construct. The paddle-chimaera channel construct was used to make a construct in which a portion of the loop connecting the S1 and S2 helices was removed (Fig. 1a, b). The amino acid residues 196–213 were replaced with three glycine residues to yield the protein sequence: DENEDGGGQSTSF. This protein was expressed and purified as described above, and was used for electrophysiology experiments.

Structure determination. Crystals were frozen in liquid nitrogen directly from their mother liquor. Diffraction data were collected to 2.4 Å at beamline X29 (Brookhaven NSLS), images were processed with DENZO, and intensities were merged with SCALEPACK[42]. Data were further processed using the CCP4 suite[43]. The crystals belong to the $P42_12$ space group. The structure was solved by molecular replacement using the program MOLREP[44], with the 2.9 Å resolution structure of rat Kv1.2 in complex with rat β2.1 subunit (PDB accession number, 2A79) as a search model. There are two channel subunits and two β subunits in the asymmetric unit, which, with crystallographic symmetry, gave rise to two four-fold tetramers (molecules 1 and 2). The tetramerization (T1) and β-subunit regions of these two tetramers are identical within the error of the coordinates. The electron density for the voltage sensors of one of the tetramers (transmembrane chain B) was significantly better defined than the other and was used to direct model building. The model was built using O[37] and was refined with CNS[38] from 50–2.4 Å to an R_{free} of 24.4%. The final model contains β2.1 residues 36–361 and paddle-chimaera channel residues 32–417. All side chains are included in the model except channel residues 133–144 (the link between T1 and the transmembrane region), which were modelled as poly-glycine. Crystallographic data and refinement statistics are shown in Supplementary Information. Figures were made using PyMol (http://www.pymol.org).

Reconstitution of Kv1.2 channels. The purified channels were reconstituted into lipid vesicles using a published procedure[45] with modifications. In brief, POPE and POPG lipid mixture (15 mg ml^{-1}:5 mg ml^{-1}, respectively, in reconstitution buffer containing 10 mM HEPES, pH 7.0, 450 mM KCl and 2 mM DTT) were solubilized with 8% octyl-β-D-maltopyranoside (Anatrace). The protein (2–10 mg ml^{-1} in gel filtration buffer, above) was then mixed with an equal volume of the solubilized lipids to yield a final protein concentration of 1–5 mg ml^{-1} and a lipid concentration of 10 mg ml^{-1}. Detergent was removed by dialyzing against reconstitution buffer with 2 mM freshly added DTT at 4 °C for 4–6 days. The resulting protein–lipid reconstitution was flash-frozen in liquid N_2 and stored at –80 °C as small aliquots.

Electrophysiological recordings. Bilayer experiments were performed as described previously[39]. In brief, planar lipid bilayers of POPE:POPG (15 mg ml^{-1}:5 mg ml^{-1}) in decane were formed by painting over a 300-μm hole in a polystyrene partition separating two aqueous chambers[40]. The chamber to which vesicles were added (*cis*) contained 4 ml of 150 mM KCl and 10 mM HEPES, pH 7.0; the opposite side (*trans*) contained 3 ml of 150 mM KCl and 10 mM HEPES (pH 7.0). Measurements were carried out using the voltage-clamp method in whole-cell mode, an Axopatch 200B amplifier, a Digidata 1322A analogue-to-digital converter and Axoclamp software (Axon Instruments) to control membrane voltage and record currents. CTX (1 μM)[41] was used to block channels in one orientation while channels in the other orientation were being recorded.

42. Otwinowski, Z. & Minor, W. Processing of X-ray diffraction data collected in oscillation mode. *Methods Enzymol.* **276,** 307–326 (1997).
43. Collaborative Computational Project. The CCP4 suite: programs for X-ray crystallography. *Acta Crystallogr. D* **50,** 760–763 (1994).
44. Vagin, A. & Teplyakov, A. An approach to multi-copy search in molecular replacement. *Acta Crystallogr. D* **56,** 1622–1624 (2000).
45. Heginbotham, L., LeMasurier, M., Kolmakova-Partensky, L. & Miller, C. Single streptomyces lividans K^+ channels: functional asymmetries and sidedness of proton activation. *J. Gen. Physiol.* **114,** 551–560 (1999).